Ashdin Publishing
Journal of Vortex Science and Technology
Vol. 1 (2012), Article ID 235591, 7 pages
doi:10.4303/jvst/235591

Research Article

Simulation of the Largest Coherent Vortices (Rolls) in the Ekman Boundary Layer

Igor Esau[1,2,3]

[1] *Nansen Environmental and Remote Sensing Centre, G.C. Rieber Climate Institute, Thormøhlens gate 47, 5006 Bergen, Norway*
[2] *Centre for Climate Dynamics, c/o Geophysical Institute, University of Bergen, Postboks 7800, 5020 Bergen, Norway*
[3] *Department of Radiophysics, University of Nizhny Novgorod, 23 Gagarin Ave., Nizhny Novgorod 603950, Russia*
Address correspondence to Igor Esau, igor.ezau@nersc.no

Received 4 June 2012; Revised 18 September 2012; Accepted 7 October 2012

Abstract Turbulence motions are often perceived as chaotic and unstructured. It has been observed however that the turbulence is frequently organized in semi-regular, persistent and large-scale coherent structures in realistic boundary layers. This study investigates such coherent structures, called rolls, in the non-stratified (Ekman) boundary layer on a rotated planet (the Earth). Large-eddy simulation numerical model is applied to reveal the roll structure, evolution and sensitivity to the flow direction and latitude. Two linearized stability mechanisms (by Lilly and by Leibovich and Lele) are considered. It was demonstrated that both mechanisms are at work in the Ekman layer but the Lilly mechanism dominate only in high latitudes whereas Leibovich and Lele mechanism dominates in low and middle latitudes. The simulation results demonstrated strong sensitivity of rolls to the wind direction. The most energetic rolls were found in low latitudes under easterly winds.

Keywords atmospheric boundary layer; large-eddy simulations; Ekman boundary layer; turbulence self-organization

1 Introduction

The turbulent planetary boundary layer is an important component of the Earth's Climate System where vertical exchange of momentum, heat and moisture is carried out by intense turbulent eddies. Practically entire biosphere and anthroposphere are confined within the planetary boundary layer. It emphasizes the importance of studies dealing with the nonlinear dynamical processes in this layer. The realistic planetary boundary layer is affected by a multitude of processes on different spatial and temporal scales. Therefore reasonable idealization of the boundary layer is necessary in its studies. One of such useful and widely used idealizations is the Ekman boundary layer.

The Ekman boundary layer (EBL) is a non-stratified turbulent boundary layer in a rotated frame of reference. The EBL was introduced to environmental science in the beginning of 20th century by V. Ekman [1] through a simple one-dimensional analytical model with a single non-dimensional number. This model did not consider the turbulence in the EBL. Turbulence was parameterized using a prescribed eddy viscosity. It is more important however that the Ekman model considered only the vertical component of the Coriolis force $f_V = 2\Omega \sin\varphi$, where Ω is the magnitude of the Earth's angular velocity and φ is the latitude of the frame of reference. The horizontal component of the force, $f_H = 2\Omega \cos\varphi$, was omitted. The Ekman model provides qualitatively correct description of the mean velocity profile, which is called the Ekman spiral, everywhere on the Earth except a narrow belt near the equator.

Satisfactory description of the mean velocity profile in the EBL does not extend to the description of the EBL turbulence. Many practically important meteorological applications, such as wind energy, precipitation, and visibility forecast, require knowledge about statistical structure of the turbulence. This problem was addressed in [6, 7, 9, 10]. It was found that solutions of the Ekman model are unstable with respect to infinitesimal perturbations. This instability results in formation of persistent longitudinal rolls. The rolls are persistent large-scale turbulent vortices with rotation axis roughly aligned with the direction of the geostrophic wind. The geostrophic wind is a free flow, which drives the EBL. There are however essentially different linearized analytical models predicting the rolls in the EBL. The Lilly model [10] (hereafter referred to as L-model) is based on the Ekman model and omits the horizontal component of the Coriolis force. The Leibovich-Haeusser-Lele model [7, 9] (hereafter referred to as LHL-model) considers both vertical and horizontal components of the force. The models' predictions of the rolls' properties are similar but not identical, which would allow us making distinction of the dynamical mechanisms structuring the turbulence in the fully nonlinear three-dimensional EBL obtained in the

Figure 1: Examples of the roll structures (cloud streets) observed in the atmosphere. Convective clouds (*Cu hum*) are located in the part of vortex with upward motions. Photos are taken by the author during his flights along the Swedish western coast in 2008–2010.

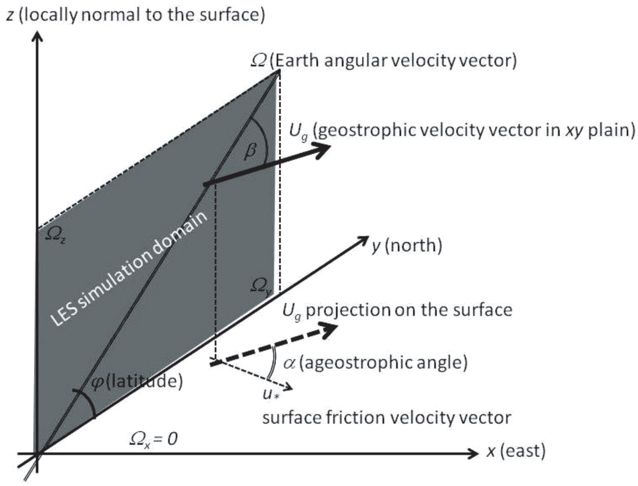

Figure 2: The coordinate system with definitions of the main vectors and angles used in the study.

LES runs. In particular, the LHL-model predicts strong dependence between the roll energy (and the spatial scale) and the geostrophic wind direction. The maximum energy is found in winds directed from east to west (the EW-winds), which are frequently observed in tropical trade wind zone below 30 degree in both hemispheres.

The rolls are a characteristic feature of the theoretical linearized EBL models but their existence in the fully nonlinear three-dimensional turbulent EBL has not been established. The difficulty is rooted in non-neutral stability of real environmental boundary layers. Figure 1 shows three examples of the atmospheric roll structures known as cloud streets. The clouds mark the updrafts in the planetary boundary layer whereas areas of downdrafts remain cloud-free. Cloud streets are frequently observed in the atmosphere but they cannot be directly associated with the EBL rolls due to buoyancy flux in clouds and at the surface. It was argued [6, 16] that the observed rolls could be amplified rather by the static but not dynamic instability in the sheared flow. In order to resolve these arguments, we employed the LES model LESNIC to simulate the neutrally stratified EBL. The LES has been already used to study the turbulence structures in the EBL. For instance, Mason and Sykes [12] simulated the EBL driven by winds from west to east (WE-winds) at mid-latitudes. Zikanov et al. [15] simulated the EBL in the equatorial ocean. Esau [2] and Huang et al. [8] simulated the EBL under a variety of control parameters and closure schemes. Unfortunately, all these runs were conducted in too small computational domains to resolve the rolls with sufficient statistical significance. A new set of LES runs in a very large computational domain was conducted for this study. These runs resolve a statistically significant number of roll vortices. Moreover, the runs were done at different latitudes and with different wind directions to address the essential distinctions between the hypothesized mechanisms of the dynamic instability in the EBL.

Thus, this study has two aims: (a) to document the development of the large-scale self-organized turbulence structures; (b) to attribute the found structures to the particular dynamical mechanism linked to the action of the Coriolis force in the model. The paper is organized in three sections and appendix. The following section describes the numerical experiments. Section 3 discusses the results. Section 4 summarizes the conclusions. Finally, the LESNIC model is described in the appendix.

2 Numerical experiments

The dimensional analysis [2] indicated that the Coriolis force impacts the most the large-scale turbulence in the EBL. Hence, the LES computational domain should be set sufficiently large to resolve a significant number of the largest turbulent vortices in the EBL. As we are looking for longitudinal rolls, we can use an advantage of the roll's homogeneity in the longitudinal direction. Hence, the LESNIC model was run in a quasi two-dimensional domain. The domain geometric size (see Figure 2) was 0.3 km in the streamwise direction, 144 km in the cross-flow direction, and 3 km in the vertical direction. The grid consists of $8 \times 4096 \times 128$ grid nodes in the corresponding directions. The small-scale turbulence was well resolved in three dimensions, whereas the large-scale turbulence was resolved only in two dimensions on the cross-flow plain. It is known [12] that the rolls will develop in this configuration of the model flow. Moreover, such configuration of the model domain is consistent with the simplifications introduced in the L- and LHL-models.

Table 1: Varied parameters, abbreviations of the LESNIC runs.

	WE-flow EBL (flow directed from West to East)	EW-flow EBL (flow directed from East to West)
The North Pole, $\varphi = 90\,°\mathrm{N}$	A0U5L90	A180U5L90
$\varphi = 60\,°\mathrm{N}$	A0U5L60	A180U5L60
$\varphi = 30\,°\mathrm{N}$	A0U5L30	A180U5L30
The Equator, $\varphi = 5\,°\mathrm{N}$	A0U5L5	A180U5L5

The conducted LES runs are listed in Table 1. Two control parameters varied: latitude and the geostrophic wind direction. The runs were integrated over 12 hours. The data were sampled every 600 s, processed and averaged over successive one-hour intervals. The geostrophic wind speed was set to $U = 5\,\mathrm{m\,s^{-1}}$.

3 Results

The LES results clearly demonstrate that the structure of the EBL turbulence varies with latitude and the geostrophic wind direction. The rolls are the major visual feature recognized in the cross-flow sections in Figures 3 and 4. The rolls are however very different in the conducted runs. Figures 3 and 4 show instant cross-flow section (the first 36 km out of the total 144 km of the cross-flow domain size) of the averaged vertical velocity component $\langle w \rangle_x$, where $\langle \cdot \rangle_x$ denotes averaging in the longitudinal direction. The rolls are very similar for EW- and WE-winds in simulations at latitude 90 °N. But as the latitude decreases, the rolls in the EW-winds gain energy and get more structured, whereas the rolls in the WE-winds loose energy and destroy.

The majority of the previous atmospheric LES were driven by the WE-wind. This is one of the possible reasons, along with authority of the L-theory, explaining the fact that the strong rolls in the low-latitude EBL have been overlooked. The simulations of the EBL with EW-wind are more interesting. They reveal that the EBL turbulence structure at latitudes less than 50 °N is determined by the energetic rolls, which occupy the entire turbulent layer. Moreover, the thickness of the turbulent layer (the EBL depth) has increased by additional mixing by the rolls. The EBL depth in the run A0U5L5 is less than 1 km while the EBL in the run A180U5L5 occupies the entire 3 km domain height. Thus, the computational domain for the EW-wind runs in low latitudes was too restrictive. It has been shown in [5] that the EBL depth can grow to 5 km and possibly higher. Between 30 °N and 60 °N there is a transition zone where the scale and energy of the rolls decrease strongly. North of 60 °N, the rolls in the WE- and EW-wind EBLs are indistinguishable and therefore they are independent of the wind direction. Figure 5 summarizes the differences in the EBL structure as dependent on latitude and the wind direction.

The normalized integrated turbulence kinetic energy (TKE) of the runs is given in Figure 6. The TKE comparison corroborates the qualitative analysis described above. In particular, it makes clear that the TKE of the coherent vortices or rolls in the EW-wind is about one order of magnitude larger than the TKE in the WE-wind in low latitudes. Figure 7 shows the evolution of the normalized TKE in the selected runs. It reveals that the observed differences are persistent during the entire time of simulations thus indicating that the rolls are long-lived features in the EBL with the time scale significantly larger than the turbulent time scales known from the literature. In the low-latitude, the TKE increases in the WE-wind significantly less than the TKE in the EW-wind EBL. It saturates after about 6 hours of simulations. By contrast, the TKE in the EW-wind EBL does not saturate during the first 12 h of simulations. An additional very long run was conducted to confirm that the TKE finally saturates after about 20 h of simulations. We suspect however that this saturation could be caused by the insufficiently large height of the domain.

Surprisingly, the difference in the TKE is not fully reflected in the geostrophic drag coefficient, $C_g = (u_*/|\vec{U}_g|)^2$. These coefficients differ by factor of 2 among the runs that correspond to the friction velocity differences by less than 50%, whereas the corresponding TKEs differ by almost one order of magnitude. Moreover, C_g does not follow the TKE growth. This behavior of the surface turbulent stress with respect to the TKE refers to the concept of inactive turbulence by Townsend [14]. According to this concept, large turbulent eddies are detached and do not exert significant turbulent stress on the surface. This is peculiar to the behavior of streaks in the non-rotated shear layer where the vortices exert a considerable fraction (20%–40%) of the total surface Reynolds stress [13].

The LES results confirmed that the EBL turbulence is organized in a set of counter-rotating longitudinal rolls. The parameters of these rolls however demonstrate a significant sensitivity to the geostrophic wind direction and latitude. This pattern of sensitivity can be summarized as follows:

(i) the roll cross-flow length scale, λ, is about 3 km. It corresponds to the EBL thickness scale, $\lambda = \delta$, so that the aspect ratio between the horizontal and vertical scales of the roll is close to unity;

(ii) the roll length scale λ is independent of altitude. This observation is inconsistent with Lin et al. [11] work, which suggests that the streak scaling should be linearly proportional to the distance from the surface;

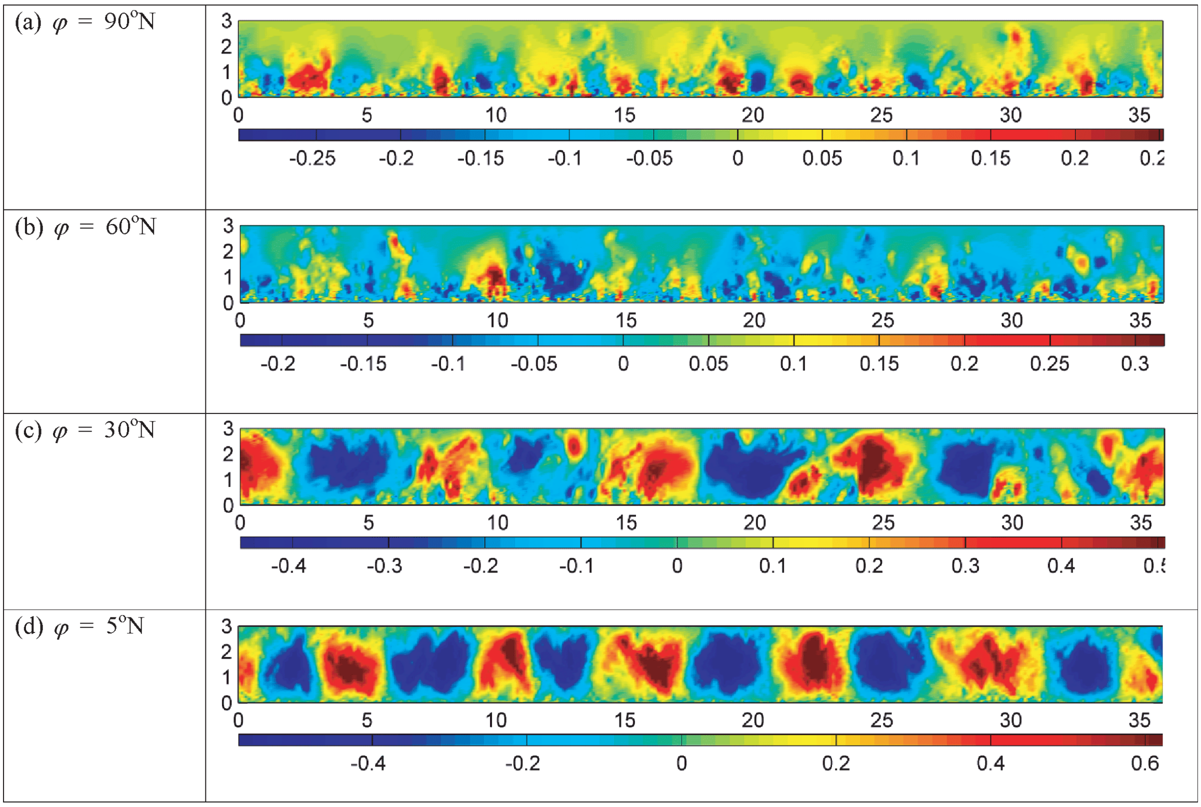

Figure 3: Coherent vortices (rolls) in the EW-flow in the EBL at different latitudes. Instant cross-flow sections of the vertical component w [$\mathrm{m\,s^{-1}}$] (color shading) of velocity averaged in the streamwise direction are shown. The distances on the y-axis (the horizontal cross-flow axis) and the z-axis (the vertical axis) are given in km. The negative values of w correspond to downward motions.

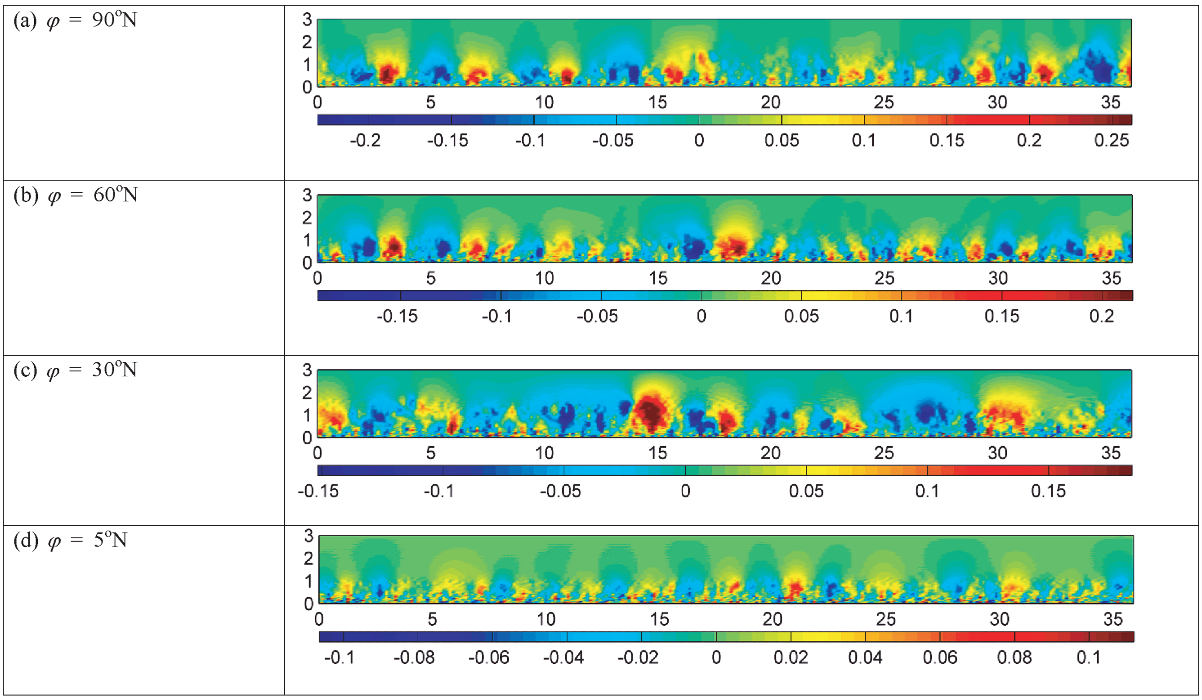

Figure 4: The same as in Figure 3 but for the WE-flow in the EBL at different latitudes.

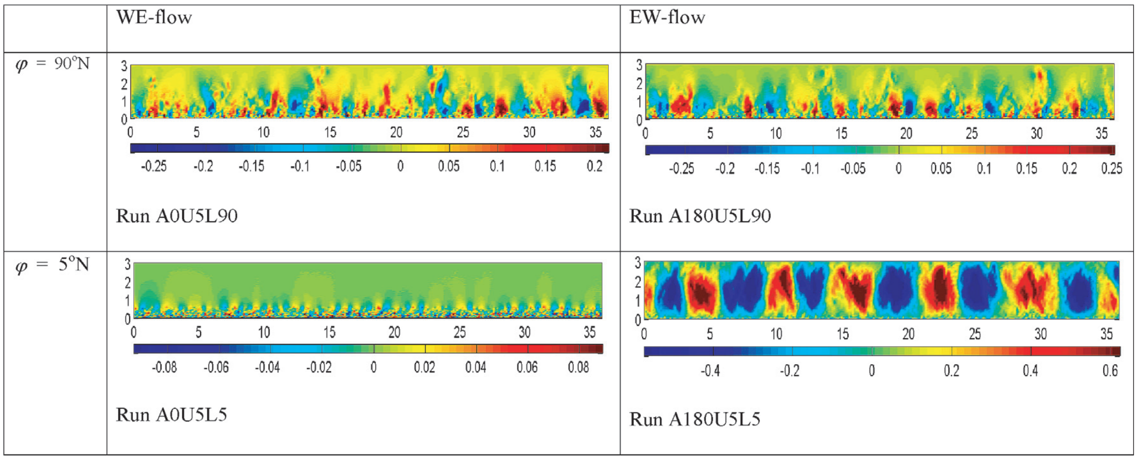

Figure 5: The same as in Figure 3 but for the comparison of the WE-flow and EW-flow EBL structures at the North Pole and near the Equator.

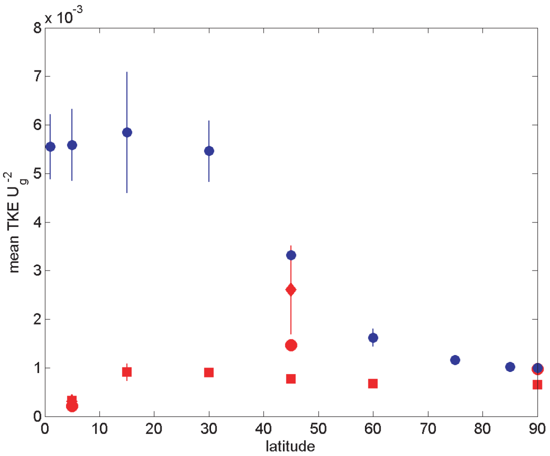

Figure 6: The mean normalized turbulent kinetic energy (TKE) in the LESNIC runs simulating the EW-flow EBL (blue dots) and WE-flow EBL (red squares). Other symbols: red dots denote the runs in a smaller but fully three-dimensional domain (512 by 128 by 128 grid nodes); red diamond—the run with the wind at 45 degrees to latitude. The vertical bars show the variability of the TKE during the EBL evolution in the corresponding runs.

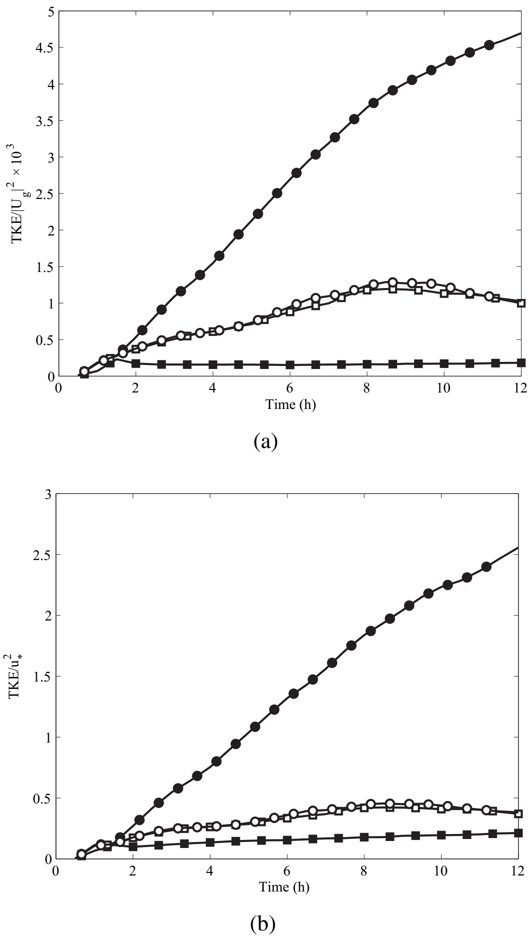

Figure 7: Temporal evolution of the domain averaged turbulent kinetic energy (TKE) normalized by (a) the module of the geostrophic velocity; (b) the surface friction velocity. The LES runs are A0U5L90 (open circles); A180U5L90 (open squares); A0U5L5 (black circles); A180U5L5 (black squares).

(iii) the turbulence in the polar EBLs is organized in less regular and less energetic vortices but it does keep some similarity to the rolls;

(iv) the turbulence in the low latitude EBL driven with WE-flow does not show recognizable large-scale vortices.

4 Conclusions

The new set of LES runs simulated the longitudinal EBL rolls in a quasi two-dimensional domain. The simulations revealed that the roll's characteristics are very different in the WE-wind and EW-wind EBL. Moreover, the simulations clearly indicated that this difference is the largest in low latitudes (south of 50 °N). These results support the LHL-model and suggest that the dynamical instability caused by the horizontal component of the Coriolis force is the mechanism responsible for the roll amplification/suppression.

At the same time, the L-model is not refuted as significant rolls were found also at high latitudes (90 °N) where only the vertical component of the Coriolis force is acting. Thus both the vertical and horizontal components of the Coriolis force lead the to formation of the longitudinal rolls in the EBL. However, the vertical component (the L-model) amplifies the rolls through destabilization of the mean velocity profile, whereas the horizontal component (the LHL-model) amplifies the rolls through direct suppression of the downscale energy cascade in turbulence.

Appendix

Large-eddy simulation model LESNIC

The complete Ekman layer model is

$$\frac{D\vec{u}}{Dt} + \nabla p' = \vec{F}_C - f_V \vec{U}_g + \vec{F}_T, \quad \mathrm{div}(\vec{u}) = 0,$$

where $\vec{U}_g$ is the geostrophic velocity and $\vec{F}_T$ is the friction force. The LESNIC model [3,4] uses a local Cartesian coordinate system (x,y,z). The orts of this system are (i,j,k). The Coriolis force is then defined as

$$\vec{F}_C = 2\vec{u} \times \vec{\Omega} = 2\begin{bmatrix} i & j & k \\ u & v & w \\ \Omega_x & \Omega_y & \Omega_z \end{bmatrix} = 2\begin{bmatrix} v\Omega_z - w\Omega_y \\ w\Omega_x - u\Omega_z \\ u\Omega_y - v\Omega_y \end{bmatrix} = \begin{bmatrix} f_V v - f_H w \\ -f_V u \\ f_H u - f_H v \end{bmatrix}.$$

Here, modules of the Coriolis force projections on the vertical, z, and horizontal, y, axes are $f_V = 2\left|\vec{\Omega}\right| \sin\varphi$ and $f_H = 2\left|\vec{\Omega}\right| \cos\varphi$, where φ is the Earth's latitude, $\vec{\Omega} = (\Omega_x, \Omega_y, \Omega_z)$ is the Earth angular velocity vector with $\Omega_x \equiv 0$, and $\vec{u} = (u,v,w)$ is the velocity vector and its projections on the coordinate axes. The velocity vector is equal to the geostrophic velocity vector above the EBL, that is $\vec{u} \to \vec{U}_g = (U_g, V_g, 0)$ at $z > h$, where h is the EBL thickness.

The turbulent stress $\vec{F}_T$ can be written in the tensor form as τ_{ij}. In the model, τ_{ij} balances the amount of energy cascading through the mesh scale, Δ, with the amount of energy cascading through some larger resolved scale, $\Delta^L > \Delta$, and thus assure the correct amount of the energy dissipation. LESNIC employs a reduced dynamic-mixed turbulence closure model as

$$\begin{aligned}
\tau_{ij} &= L_{ij}^L - 2l_s^2 \left|S_{ij}\right| S_{ij}, \\
l_s^2 &= \frac{1}{2}\frac{\left(L_{ij}^L - H_{ij}^L\right) \cdot M_{ij}^L}{M_{ij}^L \cdot M_{ij}^L}, \\
L_{ij}^L &= \left(u_i u_j\right)^L - \left(u_i\right)^L \left(u_j\right)^L, \\
H_{ij}^L &= \left(\left(\left(u_i\right)^L \left(u_j\right)^L\right)^l\right)^L - \left(\left(\left(u_i\right)^L\right)^l\right)^L \left(\left(\left(u_j\right)^L\right)^l\right)^L \\
&\quad - \left[\left(\left(u_i\right)^l\right)^L \left(\left(u_j\right)^l\right)^L - \left(\left(u_i\right)^l \left(u_j\right)^l\right)^L\right], \\
M_{ij}^L &= \left(\left|S_{ij}\right| S_{ij}\right)^L - \alpha \left|\left(S_{ij}\right)^L\right| \left(S_{ij}\right)^L, \\
S_{ij} &= \frac{1}{2}\left(\partial u_i/\partial x_j + \partial u_j/\partial x_i\right).
\end{aligned} \tag{1}$$

Here $A_i \cdot A_j$ is the scalar product, $|A_i| = (A_i \cdot A_i)^{1/2}$, the superscripts l and L denote filtering with the mesh length scale and the twice mesh length scale filters. The filters' squared aspect ratio is $\alpha = 2.92$ for the Gaussian and the top-hat filters, which are undistinguishable when discretized with central-difference schemes of the 2nd order of accuracy. The tensors in the closure (1) are as follows: L_{ij}^L is the part of τ_{ij}, which is due to interactions between the resolved scale motions only; H_{ij}^L or the cross term is the part of τ_{ij}, which describes the interactions between the resolved scales with the effect on the unresolved scales of motions; M_{ij}^L or the sub-grid term is the part of τ_{ij}, which is the interactions with the direct effect on the unresolved scales of motions; S_{ij} is the resolved velocity shear tensor. It is worth to observe that L_{ij}^L and H_{ij}^L are independent of the choice of the turbulence closure but depend on the choice of the model filter and the optimization method. The exact form of M_{ij}^L depends on the turbulence closure. LESNIC uses the 2nd order fully conservative finite-difference skew-symmetric scheme, the uniform staggered C-type mesh, and the explicit Runge-Kutta 4th-order time scheme. Their detailed description can be found in [3].

The surface boundary conditions in LESNIC are

$$\begin{aligned}
&\tau_{ij}(x,y,z=0) = \delta_{i3} u_*^2(x,y) \cdot u_i(x,y,z_1) / \left|u_i(x,y,z_1)\right|, \\
&u_*(x,y) = \kappa \left|u_i(x,y,z_1)\right| / \ln(z_1/z_0), \\
&\tau_{ij}(x,y,z=L_z) = 0, \\
&\partial u_i/\partial z\big|_{z=L_z} = 0.
\end{aligned}$$

Here, $z_0 = 0.1$ m is the surface roughness, $\kappa = 0.4$ is the von Karman constant, and L_z is the height of the domain.

Acknowledgments The research leading to these results has received funding from: the European Union's Seventh Framework Programme FP/2007-2011 under grant agreement no. 212520; the Norwegian Research Council basic research programme project PBL-feedback 191516/V30; the Norwegian Research Council project RECON 200610/S30; the European Research Council Advanced Grant, FP7-IDEAS, 227915; and a grant from the Government of the Russian Federation under Contract no. 11.G34.31.0048. The author acknowledges fruitful discussions with and support from Dr. A. Glazunov (Institute for Numerical Mathematics, Moscow, Russia) and Mr. J. Fricke (Institute for Meteorology and Climatology at Leibniz University in Hannover, Germany). The special gratitude should be given to the Bjerknes Centre for Climate Research (Bergen, Norway) and the Norwegian programme NOTUR for the generous support and funding over many years.

References

[1] V. W. Ekman, *On the influence of the Earth's rotation on ocean currents*, Ark. Mat., 2 (1905), 1–52.

[2] I. Esau, *The Coriolis effect on coherent structures in planetary boundary layers*, J. Turbul., 4 (2003), 19.

[3] I. Esau, *Simulation of Ekman boundary layers by large eddy model with dynamic mixed subfilter closure*, Environmental Fluid Mech., 4 (2004), 273–303.

[4] I. Esau and S. S. Zilitinkevich, *Universal dependences between turbulent and mean flow parameters instably and neutrally stratified Planetary Boundary Layers*, Nonlinear Processes in Geophysics, 13 (2006), 135–144.

[5] J. Fricke, *Coriolis instabilities in coupled atmosphere-ocean large-eddy simulations*, master's thesis, Institute of Meteorology and Climatology, Leibniz University of Hannover, 2011.

[6] T. Haack and H. N. Shirer, *Mixed convective—Dynamic roll vortices and their effects on initial wind and temperature profiles*, J. Atmospheric Sci., 49 (1992), 1181–1201.

[7] T. M. Haeusser and S. Leibovich, *Pattern formation in the marginally unstable Ekman layer*, J. Fluid Mech., 479 (2003), 125–144.

[8] J. Huang, M. Cassiani, and J. D. Albertson, *Analysis of coherent structures within the atmospheric boundary layer*, Boundary-Layer Meteorol., 131 (2009), 147–171.

[9] S. Leibovich and S. K. Lele, *The influence of the horizontal component of Earth's angular velocity on the instability of the Ekman layer*, J. Fluid Mech., 150 (1985), 41–87.

[10] D. Lilly, *On the instability of Ekman boundary flow*, J. Atmospheric Sci., 23 (1966), 481–494.

[11] C.-L. Lin, J. McWilliams, C.-H. Moeng, and P. Sullivan, *Coherent structures and dynamics in a neutrally stratified planetary boundary layer flow*, Phys. Fluids, 8 (1996), 2626–2639.

[12] P. J. Mason and R. I. Sykes, *A two-dimensional numerical study of horizontal roll vortices in the neutral atmospheric boundary layer*, Q. J. Roy. Meteorol. Soc., 106 (1980), 351–366.

[13] W. Schoppa and F. Hussain, *Numerical study of near-wall coherent structures and their control in turbulent boundary layers*, in Sixteenth International Conference on Numerical Methods in Fluid Dynamics (Arcachon, 1998), vol. 515 of Lecture Notes in Phys., Springer-Verlag, Berlin, 1998, 103–116.

[14] A. A. Townsend, *Equilibrium layers and wall turbulence*, J. Fluid Mech., 11 (1961), 97–120.

[15] O. Zikanov, D. N. Slinn, and M. R. Dhanak, *Large-eddy simulations of the wind-induced turbulent Ekman layer*, J. Fluid Mech., 495 (2003), 343–368.

[16] S. S. Zilitinkevich and I. Esau, *Resistance and heat-transfer laws for stable and neutral planetary boundary layers: Old theory advanced and re-evaluated*, Q. J. Roy. Meteorol. Soc., 131 (2005), 1863–1892.